Longitudinal study of sustainable acceleration of immunosenescence and immunoactivation dependent on SIV replication stress in SIVmac239-infected rhesus macaques

Jing Xue (xuejing@cnilas.org)
Institute of Laboratory Animal Science, Chinese Academy of Medical Sciences

Ling Tong
Institute of Laboratory Animal Science, Chinese Academy of Medical Sciences

Zhe Cong
Institute of Laboratory Animal Science, Chinese Academy of Medical Sciences

Long Tian
Institute of Laboratory Animal Science, Chinese Academy of Medical Sciences

Jingjing Zhang
Institute of Laboratory Animal Science, Chinese Academy of Medical Sciences

Jiahan Lu
Institute of Laboratory Animal Science, Chinese Academy of Medical Sciences

Qiuhan Lu
Institute of Laboratory Animal Science, Chinese Academy of Medical Sciences

Ting Chen
Institute of Laboratory Animal Science, Chinese Academy of Medical Sciences

Yuhong Wang
Department of Gerontology and Geriatrics, The First Affiliated Hospital of Harbin Medical University

Qiang Wei
Institute of Laboratory Animal Science, Chinese Academy of Medical Sciences

Article

Keywords: HIV/SIV, immune activation, immunosenescence, rhesus macaques, PD-1

Posted Date: March 1st, 2021

DOI: https://doi.org/10.21203/rs.3.rs-208517/v1

Abstract

It is challenging to trace the variations of host immune features covering the whole process of 'baseline-infection-treatment-withdrawal' from HIV-negative to HIV-rebound in HIV-infected patients after discontinuing antiretroviral therapy (ART). Herein, eight monkeys were monitored for 28 days to acquire baseline immune function; infected with 100 $TCID_{50}$ of SIV_{mac239} intravenously for 98 days; treated with standard ART for 90 days; followed up for 49 days post withdrawal of ART. Within the 266 days' longitudinal study, four SIV-dependent stages, SIV-negative (SN, 'baseline'), SIV-emerged (SE, 'infection'), SIV-suppressed (SS, 'treatment'), and SIV-rebounded (SR, 'withdrawal'), were stratified according to plasma viral RNA quantification. Parallel comparisons of host immune function, including counts of $CD4^+$ T cells, ratios of T-cell subsets and measurement of a panel of cytokines, were performed between SS and SN, and between SR and SE. Compared to the SN stage, an accelerated immunosenescence was found in the SS stage characterized with increased $CD38^+$ HLA-DR^- $CD4^+/CD8^+$ T-cell subsets, PD-1^+ memory $CD4^+/CD8^+$ T-cell subsets and elevated cytokines including MIP-1β, IL-8 and IL-10. Compared to the SE stage, the SR phase exhibited an accelerated immune activation against SIV characterized with increased PD-1^+ $CD4^+$ T_{CM} cells, decreased PD-1^+ $CD4^+$ T_{EM} cells and enhanced pro-inflammatory cytokine levels including TNF-α, IL-6, IL-1β and IFN-γ. This longitudinal study of rhesus macaques demonstrated a sustainable acceleration of immunosenescence/immunoactivation dependent on the stress of SIV replication which may provide insights for future HIV therapies.

Introduction

Individuals infected with HIV/SIV with or without antiretroviral treatment undergo a sustained immune activation. The characteristics of the adaptive and innate immune responses are correlated with virus persistence even in hosts that have received successful antiretroviral therapy (ART) [1, 2]. Moreover, elevated inflammation was detected in HIV patients after cessation of ART compared with healthy individuals [3, 4].

The immunologic abnormalities stemming from HIV infections persist at a low level during successful suppression of HIV replication, and this phenomenon appears similar to the immunosenescence of adaptive immunity observed as a result of normal aging [5]. During HIV/SIV replication, the host's immune system dysfunctionally responded to the replicating virus [6, 7] by activating CD38 and HLA-DR on T cells [8-10] and enhancing the cytokine cascade including TNF-α, IL-6, IL-8, IL-10, IFN-α, and IP-10 [11, 12]. During long-term antiviral therapy, sustainable inflammatory responses were still activated albeit at a low level [6, 13, 14] irrespective of the inhibition of viral replication. This chronic low-level inflammatory activation, termed 'inflammaging', is one of the attributive causes for age-related cardiovascular disease, metabolic disorders, neurocognitive decline, and cancer [12, 15, 16]. Therefore, HIV infection could be regarded as an accelerated activation triggered by detectable viral replication or an accelerated immunosenescence in the presence of undetectable viral replication [17, 18].

In the present study, systematic assessment of host-virus interaction was longitudinally performed with stage-dependent comparison along the ‘baseline-infection-treatment-withdrawal’ trajectory. The pre-infection assessment of the non-human primate model provides a baseline level of immunosenescence, which is difficult to be acquired in human HIV infections within the same individual. The profiling of accelerated immune activation against detectable viruses and accelerated immunosenescence against undetectable viruses could provide useful data in developing a functional HIV cure.

Methods

Study Design

Eight 4-6 year-old, male and female pathogen-free (SPF) rhesus monkeys (*Macaca mulatta*) were housed and cared for in accordance with the Institutional Animal Care and Use Committee (IACUC) of the Institute of Laboratory Animal Science and the recommendations of the Weatherall report for the use of non-human primates in research (http://www.acmedsci.ac.uk/more/news/the-use-of-non-human-primates-in-research/) in an Association for Assessment and Accreditation of Laboratory Animal Care (AAALAC)-accredited facility. Macaques were intravenously infected with 100 tissue culture infective doses ($TCID_{50}$) of SIV_{mac239} as described [19]. All animal procedures and experiments were performed according to protocols approved by the IACUC of the Institute of Laboratory Animal Science, Chinese Academy of Medical Sciences (No. XJ19005). All animals were anesthetized with ketamine hydrochloride (10 mg/kg) prior to sample collection and experiments were performed in a biosafety level 3 laboratory.

ART was initiated 98 days after infection and continued for three months. The ART regimen consisting of two reverse transcriptase inhibitors, 5 mg/ml tenofovir disoproxil fumarate (TDF) and 40 mg/ml emtricitabine (FTC), plus 2.5 mg/ml of the integrase inhibitor dolutegravir (DTG), was subcutaneously administered once daily at 1 ml/kg body weight [20]. The eight monkeys were followed up three months after discontinuation of ART. As part of the longitudinal observation, the effect of SIV RNA and total viral DNA on CD4 T-cell counts, immunocyte subsets and cytokines was measured at the indicated time points (**Fig. 1**).

Quantification of SIV RNA and total SIV DNA

Viral RNA (vRNA) was isolated from plasma using a QIAamp viral RNA mini kit (Qiagen, Valencia, CA, United States). Total viral DNA (vDNA) was extracted from monkey peripheral blood mononuclear cells (PBMCs) using a QIAamp blood DNA mini kit (Qiagen, Valencia, CA, United States) as previously reported [19]. Viral RNA was subjected to quantitative real-time reverse transcription-PCR (qRT-PCR) on an ABI 9700 real-time PCR system (Applied Biosystems) using the following primers and probe: Gag91 forward primer: 5¢–GCA GAG GAG GAA ATT ACC CAG TAC–3¢; Gag91 reverse primer: 5¢–CAA TTT TAC CCA GGC ATT TAA TGT T–3¢; Probe: 5’-(FAM)-ACC TGC CAT TAA GCC CGA—(MGB)-3’. The copy numbers were

estimated by comparison to a pGEM-SIV gag477 standard curve. The limits of detection were 100 copy equivalents of RNA or DNA per ml of plasma. Triplicate test reactions were performed for each sample.

Flow cytometry

Aliquots (50 µl) of EDTA-treated whole blood were stained with monoclonal antibodies to CD3 PerCP (SP34-2, BD Biosciences, 552851), CD4 FITC (OKT-4, Biolegend, 317408), and CD8 PE (RPA-T8, BD Biosciences, 555367). $CD4^+$ T-cell counts were determined with BD Trucount tubes according to the manufacturer's instructions (BD Biosciences, CA, USA). PBMCs were isolated using conventional Ficoll-Hypaque density gradient centrifugation (GE Healthcare, Uppsala, Sweden). Polychromatic flow cytometry was performed to quantitate activated $CD4^+$ or $CD8^+$ T lymphocytes (**Suppl. Fig. 1**) and $CD4^+$ or $CD8^+$ memory T lymphocyte subsets (**Suppl. Fig. 2**). Activated or memory T lymphocyte subsets (**Table 1**) from 1×10^6 PBMCs were stained with anti-CD3 BV605 (SP34-2, BD Biosciences, 562994), anti-CD4 BV711 (OKT-4, Biolegend, 317440), anti-CD8 PE (RPA-T8, BD Biosciences, 557086), anti-CCR7 BV421 (G043H7, Biolegend, 352208), anti-CD45RA APC (5H9, BD Biosciences, 561210), anti-CD38 FITC (AT-1, Stemcell, 60131FI), anti-HLA-DR BV510 (G46-6, BD Biosciences, 563083), and anti-PD-1 PerCP-cy5.5 (EH12.2H7, Biolegend, 329914) monoclonal antibodies. Cells were resuspended in 1% paraformaldehyde, subjected to flow cytometry within 24 h on a FACSAriaII (BD Biosciences, CA, U.S.) and analyzed using FlowJo V_{10} software.

Multiplex analysis using Luminex

Blood samples were centrifuged for 10 min at 600 ×g, and serum was immediately aliquoted and stored at −80°C. The following 11 cytokines were measured with a Luminex kit according to the manufacturer's instructions: IL-1β, IL-2, IL-6, IL-8, IL-10, IFN-γ, MCP-1, MIP-1β, TNF-α (Merck Millipore, Billerica, Massachusetts, USA, PRCYTOMAG-40K-09C), TGF-β (Merck Millipore, Billerica, Massachusetts, USA, PRCYTOMAG-40K-09C), and IP-10 (EPX01A-40284-901, Carlsbad, CA, USA). After thawing the samples on ice and sufficient mixing, 25 µl of supernatant was loaded into each well of a 96-well plate and mixed with 25 µl of assay buffer and 25 µl of magnetic beads. The plates were incubated with agitation overnight at 4°C. After washing, 25 µl of detection antibody was added to each well and the plate was incubated 1 h at room temperature (RT). Then, 25 µl of streptavidin-PE was added to each well and incubated for 30 min at RT. Next, 150 µl sheath fluid was added to each well after washing. Plates were read on a Luminex® 200 (Bio-Rad, CA, USA) and the data analyzed for median fluorescent intensity (MFI) using a five-parameter logistic method for calculating analyte concentration.

Statistical analysis

Comparisons between the two groups were determined using paired *t*-tests. Comparison of quantitative variables was assessed with Friedman's test. The Spearman rank test was used to determine correlations. All data were analyzed using GraphPad Prism 9.0 software (GraphPad Software Inc., San Diego, CA, United States). Significance was set at * $p \leq 0.05$, ** $p \leq 0.01$, and *** $p \leq 0.001$.

Results

Generation of the ART-treated, SIV_{mac239}-infected monkey model

Eight rhesus monkeys were intravenously infected with 100 $TCID_{50}$ SIV_{mac239}. A 3-month ART regimen consisting of daily *s.c.* injections of tenofovir (TDF), dolutegravir (DTG), and emtricitabine (FTC) was continued from 98 days post-infection (dpi), with a 49-day follow-up after stopping ART. During the observation periods, the levels of viral RNA and total viral DNA were measured, together with counts of $CD4^+$ T cells and ratios of immunocyte subsets, and quantitation of cytokine levels (**Fig. 1**). Data collection for the model was divided into four stages: baseline (pre-infection), infection, treatment, and withdrawal based on the variation of vRNA replication (**Fig. 2a**). With regard to virus, at baseline stage, SIV was negative (SN, 'baseline'); after acute and chronic SIV infection, SIV emerged (SE, 'infection') with a peak plasma SIV RNA level of 6.91 log_{10} copies/ml (range 5.75-7.58 log_{10} RNA copies/ml); during ART, the SIV replication was suppressed (SS, 'treatment') to undetectable levels (limits of detection, 2.00 log_{10} RNA copies/ml); after cessation of ART, the SIV RNA rebounded (SR, 'withdrawal') with the peak of plasma viral RNA ranging from 4.60 to 6.99 log_{10} RNA copies/ml. The longitudinal vDNA ranged from 3.20 to 3.90 log_{10} vDNA copies/ml after acute SIV infection. The vDNA in the SR phase was significantly lower than in the SE phase (SR vs SE, $p = 0.0009$) (**Fig. 2b, right panel**).

The $CD4^+$ T-cell counts and CD4/CD8 ratios were compared to determine the status of immune reconstitution. $CD4^+$ T-cell counts during ART (SS phase) were slightly increased, but differences were not significant (SS vs SE, $p = 0.4044$; and SS vs SR, $p = 0.8061$) (**Fig. 2c**). CD4/CD8 ratios in the SS phase were significantly increased compared with those during SE (SS vs SE, $p = 0.0017$) and in the SR phase (SS vs SR, $p = 0.0128$), which returned to the normal level before infection (SS vs SN, $p = 0.4280$) (**Fig. 2d**).

Significant increase in activated or PD-1-expressing T cells with elevated levels of inflammatory cytokines in SS vs SN

Ratios of $CD38^+$ $HLA\text{-}DR^-$ $CD4^+$ ($p = 0.0027$) / $CD8^+$ ($p = 0.0373$) T-cell subsets in the SS phase were significantly higher than in SN before infection (**Fig. 3a**). No significant difference was shown in $CD38^+$ $HLA\text{-}DR^+$, $CD38^-$ $HLA\text{-}DR^+$ or $CD38^-$ $HLA\text{-}DR^-$ activated $CD4^+/CD8^+$ T-cell subsets between SS and SN phases ($p > 0.05$). For memory $CD4^+/CD8^+$ T-cell subsets, $CD4^+/CD8^+$ T_{CM}, $T_{Naïve}$, T_{EMRA} or T_{EM} during ART (SS) were not significantly different compared to those in SN (**Fig. 3b**). There was a significant

increase in PD-1-expressing T-cell subsets during SS including PD-1^+/$CD4^+$ T_{CM} (p = 0.0018) and PD-1^+/$CD4^+$ T_{EM} (p = 0.0165) (**Fig. 3c,** *left panel*) as well as PD-1^+/$CD8^+$ T_{CM} (p = 0.0270) and PD-1^+/$CD8^+$ T_{EM} (p = 0.0106) (**Fig. 3c,** *right panel*) compared to before infection. Serum profiles of anti- and pro-inflammatory cytokines and chemokines were compared between SS and SN (**Suppl. Fig. 3)**. IL-10 (p = 0.0482), IL-8 (p = 0.0040) and MIP-1β (p = 0.0080) were significantly elevated in SS compared to SN phase (**Fig. 3d**).

Significant shift in PD-1-activated T cells with elevated inflammatory cytokines in relation to SIV replication in SR vs SE

Comparing SR to SE, we found no significant difference in activated $CD4^+$/$CD8^+$ T-cell subsets with CD38 and/or HLA-DR expression (**Fig. 4a**) as well as memory T-cell subsets with CCR7 and/or CD45RA expression (**Fig. 4b**) (p > 0.05). The only significant changes were an increase in PD-1^+ $CD4^+$ T_{CM} cells (p = 0.0110) and decrease in PD-1^+ $CD4^+$ T_{EM} cells (p = 0.0466) in SR compared to SE (**Fig. 4c,** *left panel*). IFN-γ (p = 0.0234), IL-1β (p = 0.0169), IL-6 (p = 0.0164) and TNF-α (p = 0.0435) were significantly elevated in SR compared to SE (**Fig. 4d**).

Systematic comparison of the level of inflammation in ART-treated SIV_{mac239}-infected macaques

Percentages of specific immune cells and cytokine levels in the four phases of 'baseline-infection-treatment-withdrawal' were systematically compared in SN vs SS and SE vs SR (**Fig. 5a)**. The frequency of immunocyte types and cytokine expression levels were compared among the four stages (**Fig. 5b**). Activated $CD4^+$ T-cell subsets with high expression of CD38 and/or HLA-DR as well as memory $CD4^+$/$CD8^+$ T-cell subsets with high expression of PD-1 were consistently sustained from stage to stage.

Discussion

We established a non-human primate model using the monkey retrovirus, SIV_{mac239}, to investigate the effects of viral replication and persistence after ART on the host immune response. Using eight SIV_{mac239}-infected rhesus macaques, we longitudinally tracked host immunosenescence and immunoactivation by comparing SS to SN and SR to SE. Our findings were consistent with previous studies[21-28], and comparing SS to SN, we showed accelerated host immunosenescence and elevated low-level inflammation at the same time as SIV expression was undetectable. In comparing SR to SE, we showed accelerated host immunoactivation with elevated inflammation that correlated with increased SIV replication during rebound [29, 30].

We found significantly elevated $CD38^+$ $HLA\text{-}DR^-$ activated $CD4^+/CD8^+$ T-cell subsets and $PD\text{-}1^+$ memory $CD4^+/CD8^+$ T-cell subsets as well as IL-10, IL-8 and MIP-1β in SS vs SN phase (**Fig. 3e**). We hypothesize that elevated expression of CD38 contributes to the increased production of the cytokines, MIP-1β, IL-8 and IL-10. ART could depress the peripheral cytokine storm [26, 31] to a very low level similar to baseline [26, 32, 33]. The continuing high expression of the chemokines, MIP-1β and IL-8, together with the anti-inflammatory factor, IL-10, were supposed to act against latency. Memory $CD4^+$ T-cells are one of the key HIV reservoirs, and PD-1 is thought to play an essential role in the establishment and maintenance of HIV latency [34]. Increased expression of PD-1 by memory $CD4^+/CD8^+$ T-cell subsets during ART suppression comparing to baseline verified the accelerated immunosenescence attributed to HIV latency.

We also found an increase in $PD\text{-}1^+$ $CD4^+$ T_{CM} cells and proinflammatory cytokine levels in SR vs SE (**Figure 4e**). $CD8^+$ T_{EM} cells appeared to be involved in the elimination of SIV-infected cells and reduced SIV transmission [31]. The increase in $PD\text{-}1^+$ $CD4^+$ T_{CM} cells accompanied by a small decrease in $PD\text{-}1^+$ $CD4^+$ T_{EM} cells might be attributed to the exhausted $CD8^+$ T_{EM} cells against HIV latency. T cell activation after ART discontinuation required TNF-α, IL-6 and IFN-γ [24, 25, 35], which is consistent with our findings.

In summary, our longitudinal study on rhesus macaques with SIV infection and ART demonstrated a sustained cellular and humoral immune response with distinct profiling both under conditions of SIV replication and latency. The sustained high expression of PD-1 might offer a potential target for treating HIV infection.

Declarations

Acknowledgements

Funding: This work was supported by the National Natural Science Foundation of China (81971944 to J.X.), the CAMS Innovation Fund for Medical Sciences (2017-I2M-1-014 to Q.W.) and the National Megaprojects of China for Major Infectious Diseases (2017ZX10304402 and 2018ZX10101001 to J.X., 2018ZX10301103 to Z.C.). **Author contributions:** Conceptualization: J.X.; Methodology: Z.C. and Ling.Tong.; Investigation: Ling.Tong., Z.C., Long.Tian., J.Z., J.L., Q.L., and T.C.; Statistical analysis: Ling.Tong., and Y.W.; Writing – Original Draft: Ling.Tong, and J.X.; Writing –Review and Editing: J.X.; Funding Acquisition: J.X., Q.W. and Z.C.; Resources: J.X., and Q.W.; Supervision: J.X., and Q.W.

Conflicts of interest

There are no conflicts of interest.

References

1. Jain, V. et al. Antiretroviral therapy initiated within 6 months of HIV infection is associated with lower T-cell activation and smaller HIV reservoir size. *The Journal of infectious diseases* **208**, 1202-1211 (2013).
2. Chun, T.W. et al. Relationship between residual plasma viremia and the size of HIV proviral DNA reservoirs in infected individuals receiving effective antiretroviral therapy. *The Journal of infectious diseases* **204**, 135-138 (2011).
3. French, M.A., King, M.S., Tschampa, J.M., da Silva, B.A. & Landay, A.L. Serum immune activation markers are persistently increased in patients with HIV infection after 6 years of antiretroviral therapy despite suppression of viral replication and reconstitution of CD4+ T cells. *The Journal of infectious diseases* **200**, 1212-1215 (2009).
4. Neuhaus, J. et al. Markers of inflammation, coagulation, and renal function are elevated in adults with HIV infection. *The Journal of infectious diseases* **201**, 1788-1795 (2010).
5. Deeks, S.G. HIV infection, inflammation, immunosenescence, and aging. *Annual review of medicine* **62**, 141-155 (2011).
6. Douek, D.C. Immune activation, HIV persistence, and the cure. *Topics in antiviral medicine* **21**, 128-132 (2013).
7. Paiardini, M. & Müller-Trutwin, M. HIV-associated chronic immune activation. *Immunological reviews* **254**, 78-101 (2013).
8. Ndhlovu, Z.M. et al. Magnitude and Kinetics of CD8+ T Cell Activation during Hyperacute HIV Infection Impact Viral Set Point. *Immunity* **43**, 591-604 (2015).
9. Chen, P. et al. Perturbations of Monocyte Subsets and Their Association with T Helper Cell Differentiation in Acute and Chronic HIV-1-Infected Patients. *Frontiers in immunology* **8**, 272 (2017).
10. Hua, S. et al. Potential role for HIV-specific CD38-/HLA-DR+ CD8+ T cells in viral suppression and cytotoxicity in HIV controllers. *PloS one* **9**, e101920 (2014).
11. Kazer, S.W., Walker, B.D. & Shalek, A.K. Evolution and Diversity of Immune Responses during Acute HIV Infection. *Immunity* **53**, 908-924 (2020).
12. van den Dries, L., Claassen, M.A.A., Groothuismink, Z.M.A., van Gorp, E. & Boonstra, A. Immune activation in prolonged cART-suppressed HIV patients is comparable to that of healthy controls. *Virology* **509**, 133-139 (2017).
13. Siewe, B. & Landay, A. in Encyclopedia of AIDS. (eds. T.J. Hope, D.D. Richman & M. Stevenson) 241-248 (Springer New York, New York, NY; 2018).
14. Siewe, B. & Landay, A. Cellular and Soluble Immune Activation Markers in HIV-Infected Subjects.
15. Hansson, G.K. Inflammation, atherosclerosis, and coronary artery disease. *The New England journal of medicine* **352**, 1685-1695 (2005).
16. Deeks, S.G., Lewin, S.R. & Havlir, D.V. The end of AIDS: HIV infection as a chronic disease. *Lancet (London, England)* **382**, 1525-1533 (2013).

17. Sokoya, T., Steel, H.C., Nieuwoudt, M. & Rossouw, T.M. HIV as a Cause of Immune Activation and Immunosenescence. *Mediators of inflammation* **2017**, 6825493 (2017).
18. Deeks, S.G., Verdin, E. & McCune, J.M. Immunosenescence and HIV. *Current opinion in immunology* **24**, 501-506 (2012).
19. Chong, H. et al. Monotherapy with a low-dose lipopeptide HIV fusion inhibitor maintains long-term viral suppression in rhesus macaques. *PLoS pathogens* **15**, e1007552 (2019).
20. Whitney, J.B. et al. Prevention of SIVmac251 reservoir seeding in rhesus monkeys by early antiretroviral therapy. *Nature communications* **9**, 5429 (2018).
21. Hunt, P.W. HIV and inflammation: mechanisms and consequences. *Current HIV/AIDS reports* **9**, 139-147 (2012).
22. Wittkop, L. et al. Effect of cytomegalovirus-induced immune response, self antigen-induced immune response, and microbial translocation on chronic immune activation in successfully treated HIV type 1-infected patients: the ANRS CO3 Aquitaine Cohort. *The Journal of infectious diseases* **207**, 622-627 (2013).
23. Antar, A.A. et al. Longitudinal study reveals HIV-1-infected CD4+ T cell dynamics during long-term antiretroviral therapy. *The Journal of clinical investigation* **130**, 3543-3559 (2020).
24. Vandergeeten, C., Fromentin, R. & Chomont, N. The role of cytokines in the establishment, persistence and eradication of the HIV reservoir. *Cytokine & growth factor reviews* **23**, 143-149 (2012).
25. Osuji, F.N., Onyenekwe, C.C., Ahaneku, J.E. & Ukibe, N.R. The effects of highly active antiretroviral therapy on the serum levels of pro-inflammatory and anti-inflammatory cytokines in HIV infected subjects. *Journal of biomedical science* **25**, 88 (2018).
26. Bordoni, V. et al. Impact of ART on dynamics of growth factors and cytokines in primary HIV infection. *Cytokine* **125**, 154839 (2020).
27. Hunt, P.W. et al. Relationship between T cell activation and CD4+ T cell count in HIV-seropositive individuals with undetectable plasma HIV RNA levels in the absence of therapy. *The Journal of infectious diseases* **197**, 126-133 (2008).
28. Yero, A. et al. Differential Dynamics of Regulatory T-Cell and Th17 Cell Balance in Mesenteric Lymph Nodes and Blood following Early Antiretroviral Initiation during Acute Simian Immunodeficiency Virus Infection. *Journal of virology* **93** (2019).
29. Molina-Pinelo, S. et al. Premature immunosenescence in HIV-infected patients on highly active antiretroviral therapy with low-level CD4 T cell repopulation. *The Journal of antimicrobial chemotherapy* **64**, 579-588 (2009).
30. Robbins, G.K. et al. Incomplete reconstitution of T cell subsets on combination antiretroviral therapy in the AIDS Clinical Trials Group protocol 384. *Clinical infectious diseases : an official publication of the Infectious Diseases Society of America* **48**, 350-361 (2009).
31. Hansen, S.G. et al. Effector memory T cell responses are associated with protection of rhesus monkeys from mucosal simian immunodeficiency virus challenge. *Nature medicine* **15**, 293-299 (2009).

32. Sereti, I. et al. Persistent, Albeit Reduced, Chronic Inflammation in Persons Starting Antiretroviral Therapy in Acute HIV Infection. *Clinical infectious diseases : an official publication of the Infectious Diseases Society of America* **64**, 124-131 (2017).
33. Casetti, R. et al. HIV-Specific CD8 T Cells Producing CCL-4 Are Associated With Worse Immune Reconstitution During Chronic Infection. *Journal of acquired immune deficiency syndromes (1999)* **75**, 338-344 (2017).
34. Evans, V.A. et al. Programmed cell death-1 contributes to the establishment and maintenance of HIV-1 latency. *AIDS (London, England)* **32**, 1491-1497 (2018).
35. Regidor, D.L. et al. Effect of highly active antiretroviral therapy on biomarkers of B-lymphocyte activation and inflammation. *AIDS (London, England)* **25**, 303-314 (2011).

Table

Table 1. Polychromatic flow cytometry for staining of T lymphocyte subsets.

T lymphocyte subsets	Biomarker
Activated T cells	$CD4^+/CD8^+$ $CD38^+$ $HLA\text{-}DR^+$
	$CD4^+/CD8^+$ $CD38^+$ $HLA\text{-}DR^-$
	$CD4^+/CD8^+$ $CD38^-$ $HLA\text{-}DR^+$
	$CD4^+/CD8^+$ $CD38^-$ $HLA\text{-}DR^-$
Naïve T cells (T_{Naive})	$CD3^+$ $CD4^+/CD8^+$ $CCR7^+$ $CD45RA^+$
$PD\text{-}1^+$ T_{Naive}	$CD3^+$ $CD4^+/CD8^+$ $CCR7^+$ $CD45RA^+$ $PD\text{-}1^+$
Central memory T cells (T_{CM})	$CD3^+$ $CD4^+/CD8^+$ $CCR7^+$ $CD45RA^-$
$PD\text{-}1^+$ T_{CM}	$CD3^+$ $CD4^+/CD8^+$ $CCR7^+$ $CD45RA^-$ $PD\text{-}1^+$
Effector memory RA^+ T cells (T_{EMRA})	$CD3^+$ $CD4^+/CD8^+$ $CCR7^-$ $CD45RA^+$
$PD\text{-}1^+$ T_{EMRA}	$CD3^+$ $CD4^+/CD8^+$ $CCR7^-$ $CD45RA^+$ $PD\text{-}1^+$
Effective memory T cells (T_{EM})	$CD3^+$ $CD4^+/CD8^+$ $CCR7^-$ $CD45RA^-$
$PD\text{-}1^+$ T_{EM}	$CD3^+$ $CD4^+/CD8^+$ $CCR7^-$ $CD45RA^-$ $PD\text{-}1^+$

Figures

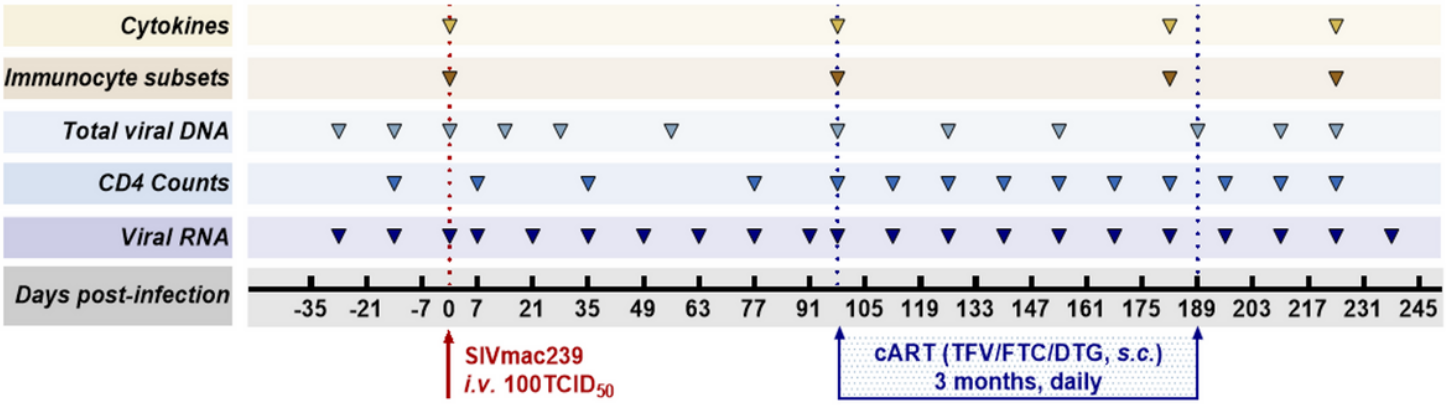

Figure 1

Study design. Eight Chinese-origin rhesus macaques were intravenously (i.v.) inoculated with 100 median tissue culture infectious doses (TCID50) of SIVmac239. At 98 dpi, ART (FTC/DTG/TDF) was administered for three months. ART was discontinued at 189 dpi with a one-month follow-up. Peripheral blood was collected to measure viral RNA, CD4 T-cell counts, total viral DNA, immunocyte subsets and cytokines at the indicated time points during the observation period.

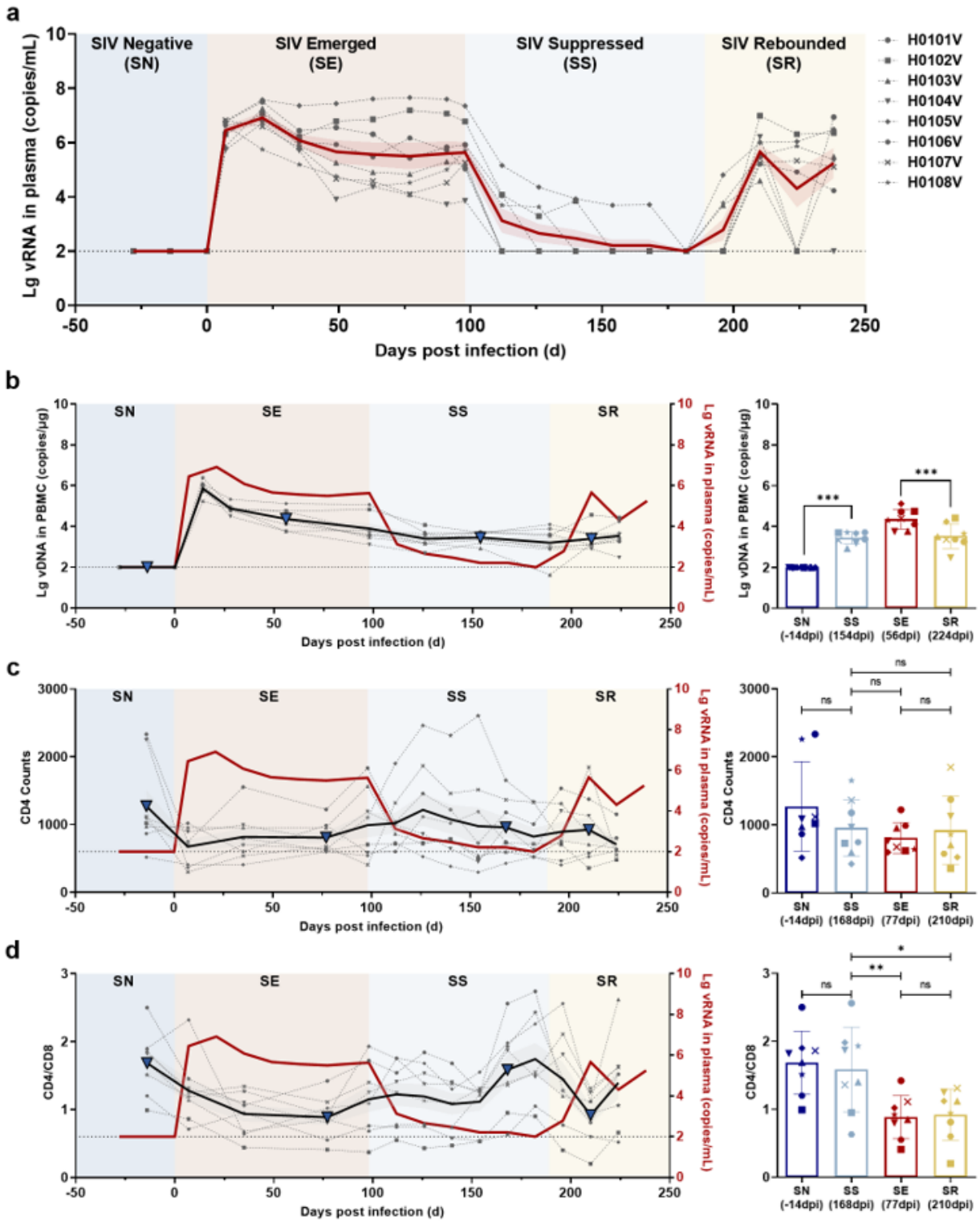

Figure 2

Dynamics of viral RNA, viral DNA, CD4 T-cell counts and CD4/CD8 ratio in ART-treated, SIVmac239-infectecd macaques. a, Dynamics of viral RNA replication. The observation period was divided into four phases according to viral replication: SIV negative (SN), SIV emerged (SE), SIV suppressed (SS), and SIV rebounded (SR). The gray dotted lines indicate the changes in viral RNA in each monkey; the red solid line, the average of viral loads for all monkeys; the red shaded area, the SEM of viral loads for all monkeys. b-

d, Dynamics of total viral DNA, CD4 T-cell counts, and CD4/CD8 ratio during the observation period. Left panel, the changes in b total viral DNA, c CD4 T-cell counts, and d CD4/CD8 ratio during the four phases (gray dotted line, changes in each monkey; black solid line, the average of all monkeys; grey shaded areas, the SD of all monkeys; red solid line, the average viral loads of all monkeys). Right panel, comparisons among SIV negative (SN), SIV emerged (SE), SIV suppressed (SS) and SIV rebounded (SR). The blue triangles in the left panel represent the time points in the right panel.

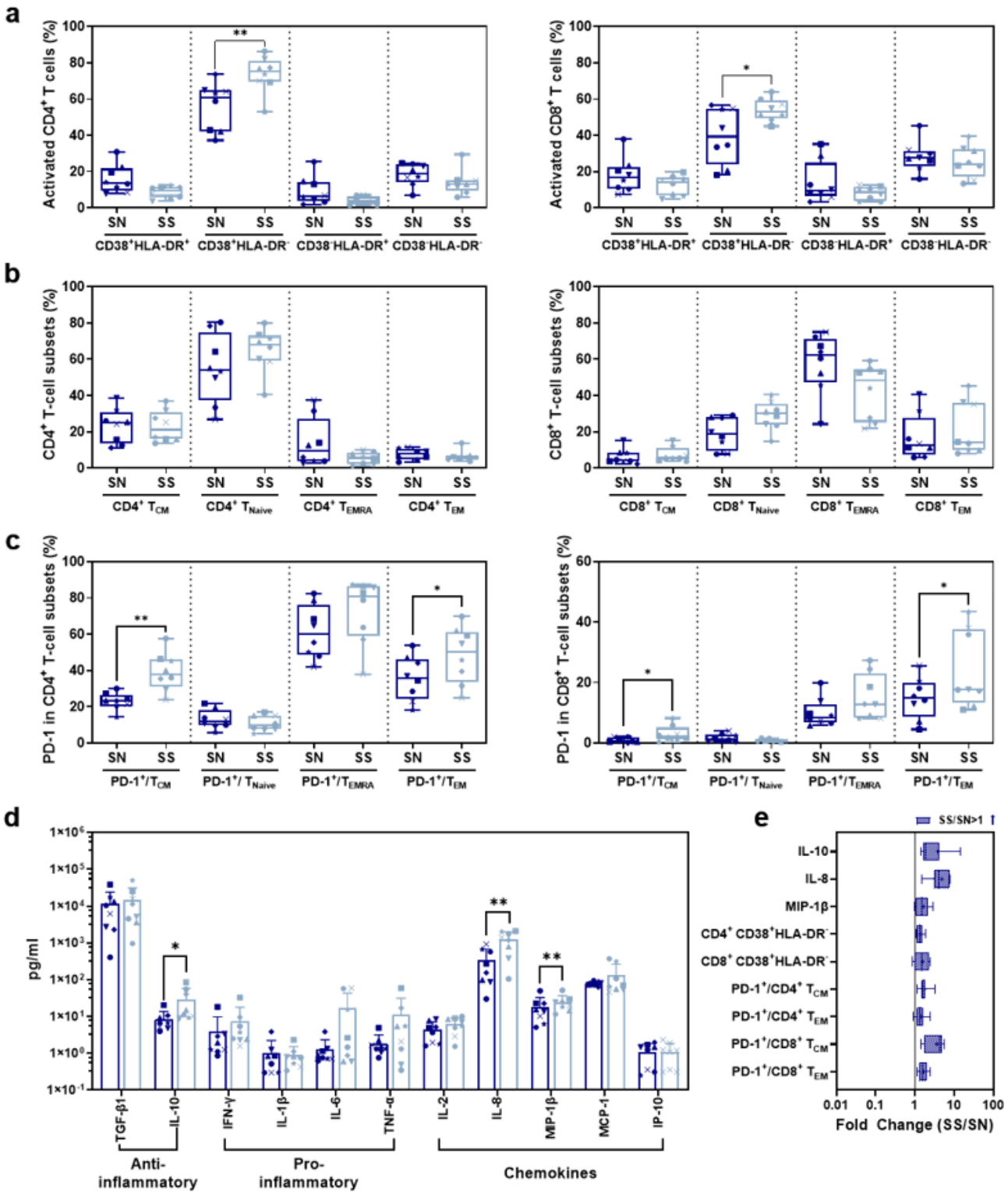

Figure 3

Comparison of CD4+/CD8+ T-cell subsets and cytokines between SS and SN phases. a, Comparison of activated CD4+ (left panel) and CD8+ (right panel) T-cell subsets from PBMC in SS vs SN. b, Comparison of CD4+ (left panel) and CD8+ (right panel) memory T-cell subsets from PBMC in SS vs SN. The percentage of central memory CD4+/CD8+ T cells (CD4+/CD8+ TCM, CD3+ CD4+/CD8+ CCR7+ CD45RA−), naive CD4+/CD8+ T cells (CD4+/CD8+ TNaive, CD3+ CD4+/CD8+ CCR7+ CD45RA+), TEMRA cells (CD4+/CD8+ TEMRA, CD3+ CD4+/CD8+ CCR7− CD45RA+), and effective memory T cells (CD4+/CD8+ TEM, CD3+ CD4+/CD8+ CCR7− CD45RA−) were compared between SS and SN phases (paired t-test, $p > 0.05$). c, Comparison of percentages of PD-1+ cells in memory T-cell subsets in SS vs SN. Left panel, comparison of percentages of PD-1+ cells in CD4+ TCM, TNaive, TEMRA, and TEM cells; right panel, comparison of percentages of PD-1+ cells in CD8+ TCM, TNaive, TEMRA, and TEM cells. d, Comparison of anti- and pro-inflammatory cytokines and chemokines between SS and SN phases. e, Fold change of cytokines and T-cell subsets with significant differences (SS value/SN value; blue filled patterns represent increased values). Data are the mean ± SD from three independent experiments. (* $p < 0.05$, ** $p < 0.01$, paired t-test, SS vs SN)

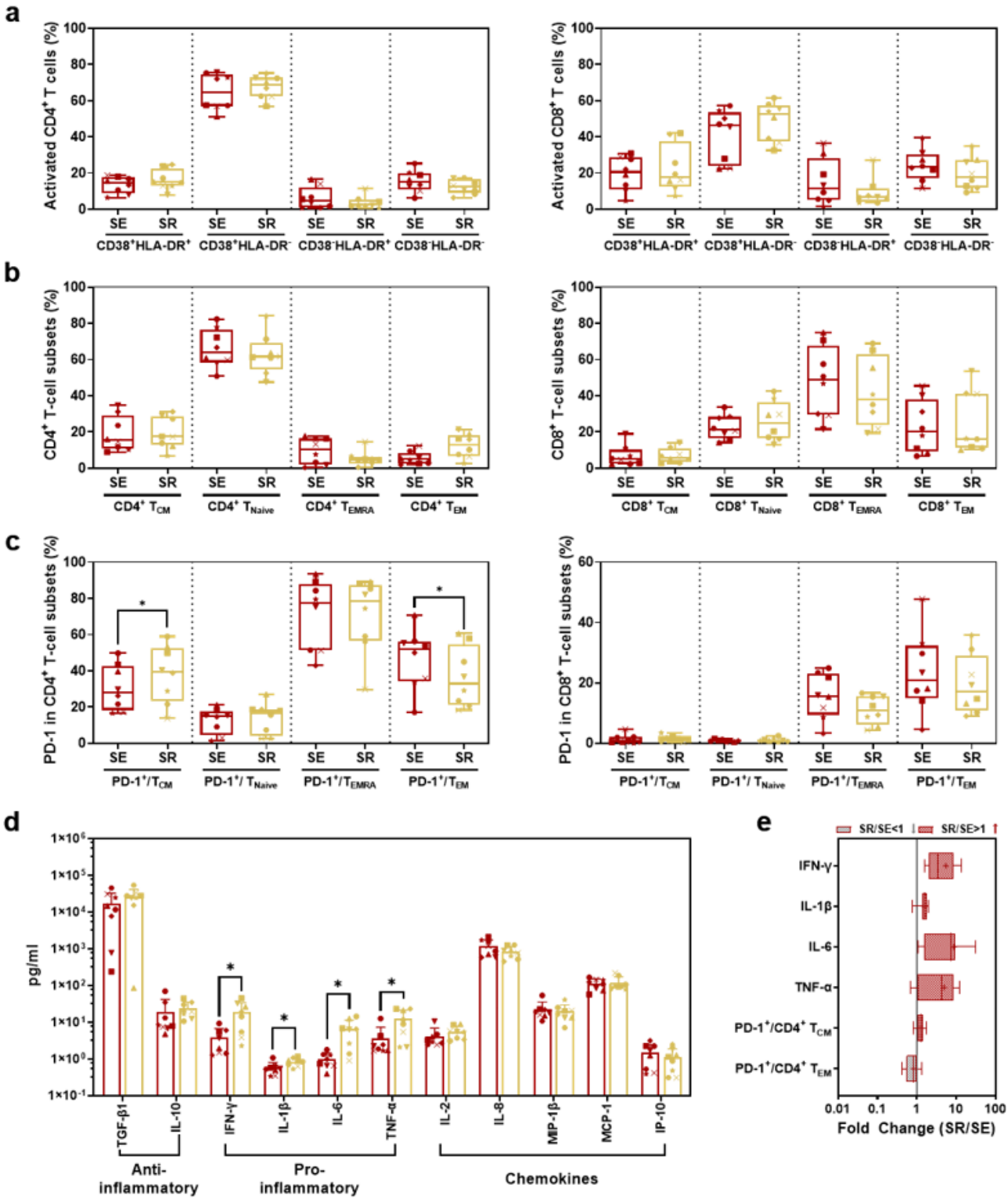

Figure 4

Comparison of CD4+/CD8+ T-cell subsets and cytokines between SR and SE phases. a, Comparison of activated CD4+ (left panel) and CD8+ (right panel) T-cell subsets from PBMC in SR vs SE. b, Comparison of CD4+ (left panel) and CD8+ (right panel) memory T-cell subsets from PBMCs in SR vs SE. The percentage of central memory CD4+/CD8+ T cells (CD4+/CD8+ TCM, CD3+ CD4+/CD8+ CCR7+ CD45RA−), naive CD4+/CD8+ T cells (CD4+/CD8+ TNaive, CD3+ CD4+/CD8+ CCR7+ CD45RA+), TEMRA

cells (CD4+/CD8+ TEMRA, CD3+ CD4+/CD8+ CCR7− CD45RA+), and effective memory T cells (CD4+/CD8+ TEM, CD3+ CD4+/CD8+ CCR7− CD45RA−) were compared between SR and SE phases (paired t-test, p > 0.05). c, Comparison of percentages of PD-1+ cells in memory T-cell subsets in SR vs SE. Left panel, comparison of percentages of PD-1+ cells in CD4+ TCM, TNaive, TEMRA, and TEM cells; right panel, comparison of percentages of PD-1+ cells in CD8+ TCM, TNaive, TEMRA, and TEM cells. d, Comparison of anti- or pro- inflammatory cytokines and chemokines between SR and SE phases. e, The fold change of cytokines and T-cell subsets with the significant differences (SR value/SE value; red-filled patterns are the increased values, and grey-filled patterns are the decreased values). Data are mean ± SD from three independent experiments. (* p < 0.05, ** p < 0.01, paired t-test, SR vs SE)

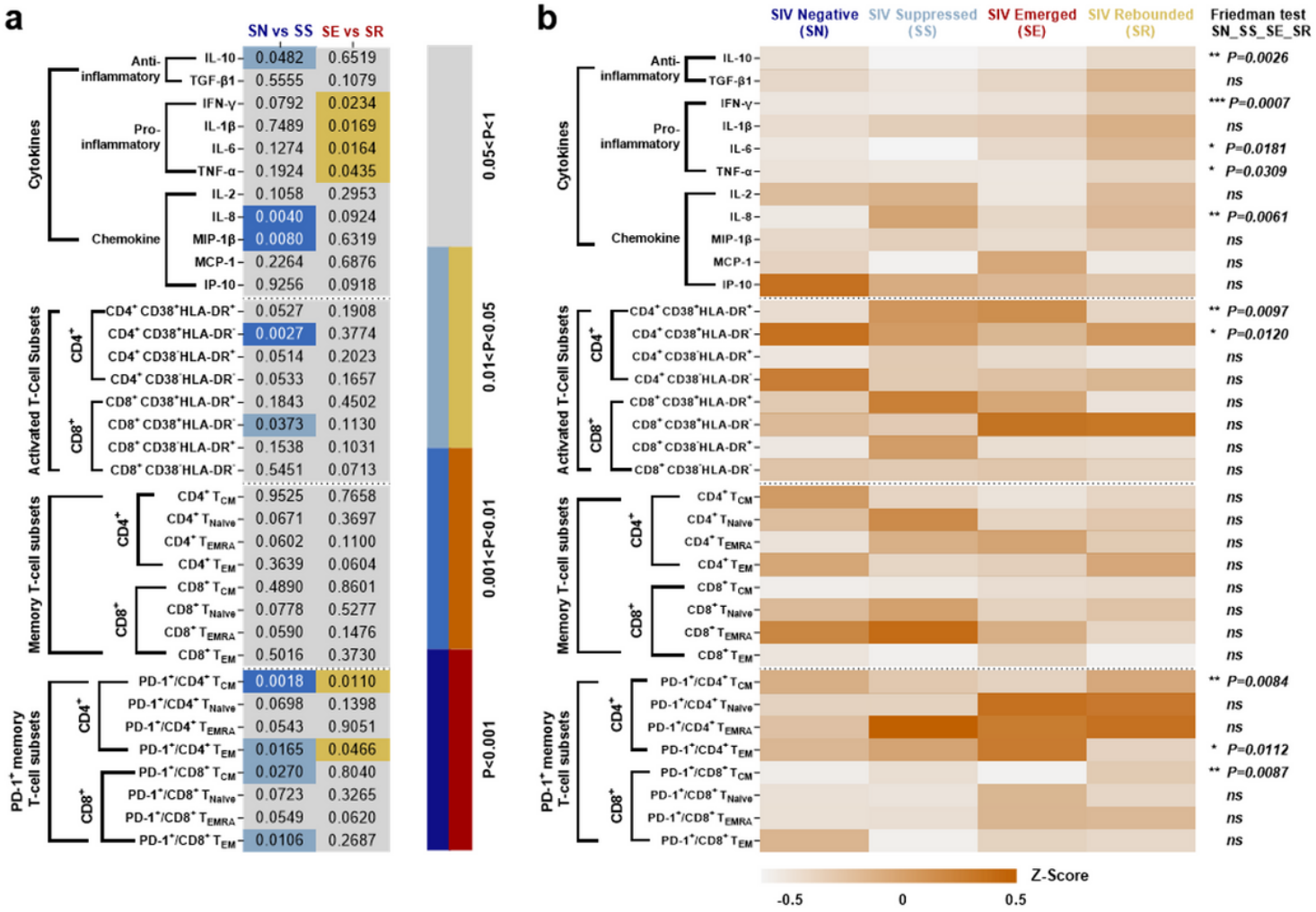

Figure 5

Systematic comparison of immune features in ART-treated, SIVmac239-infectecd macaques. a, p values of immunocyte subsets and cytokines in SS vs SN and SR vs SE. b, Expression pattern of immunocyte subsets and cytokines during SN, SS, SE and SR phases. All data are standardized by z-score and analyzed by Friedman matched paired test (* p < 0.05; ** p < 0.01; *** p < 0.001; ns, not significant).

Supplementary Files

This is a list of supplementary files associated with this preprint. Click to download.

- SupportingInformation.docx